TECHNICAL TRANSACTIONS 11/2018
ELECTRICAL ENGINEERING
DOI: 10.4467/2353737XCT.18.167.9423
SUBMISSION OF THE FINAL VERSION: 11/10/2018

Marek Dudzik
marekdudzik@pk.edu.pl
Janusz Prusak
Faculty of Electrical and Computer Engineering, Cracow University of Technology
Sławomir Drapik
ELECTREN S.A.
Valeriy Kuznetsov
Dniepropetrovsk National University of Railway Transport (DIIT), Ukraine

The efficiency of using artificial feedforward neural networks with a single hidden layer of eight neurons for the analysis of overload conditions of selected tramway traction substations

Efektywność wykorzystania sztucznych sieci neuronowych, typu feedforward o jednej warstwie ukrytej ośmio-neuronowej, do analizy przeciążeń wybranej tramwajowej podstacji trakcyjnej

Abstract

This paper presents further results of research on the load variability of rectifier units for the selected tram traction substation. Actual measurements were used in the performed analysis. This time, the analysis was focused on the characteristics of maximum loads and overloads for time periods of five minutes and sixty minutes, for a number of selected cases. The second part of the article discusses the effectiveness of the use of artificial neural networks of the feedforward type with one hidden layer with eight neurons to analyse the overloads of the traction substation over a longer time scale. The obtained positive results indicate that this type of research should be continued, using different variants of artificial neural networks.

Keywords: loads and overloads of tram traction substation, artificial neural network

Streszczenie

W artykule przedstawiono kolejne wyniki badań zmienności obciążeń zespołów prostownikowych wybranej tramwajowej podstacji trakcyjnej. Do analiz wykorzystano rzeczywiste wyniki pomiarów. Tym razem zwrócono uwagę na specyfikę maksymalnych obciążeń i przeciążeń w odcinkach czasowych 5 min i 60 min – dla kilku wybranych przypadków. W drugiej części artykułu przedstawiono efektywność wykorzystania sztucznych sieci neuronowych, typu feedforward o jednej warstwie ukrytej z ośmioma neuronowami, do analizy przeciążeń dla eksploatacji podstacji trakcyjnej w dłuższej skali czasowej. Uzyskane pozytywne wyniki wskazują na konieczność kontynuowania tego typu badań, m.in. wykorzystując inne warianty sztucznych sieci neuronowych.

Słowa luczowe: obciążenia i przeciążenia tramwajowej podstacji trakcyjnej, sztuczne sieci neuronowe

1. Introduction

Rectifier systems in tramway traction substations undergo varying loads [3, 15, 20]. The studies conducted by the authors [1, 2, 4, 6–8, 16, 17] have confirmed this hypothesis. It has also been found that DC power supply systems of the electric traction have some power redundancy resulting from the required overrating e.g. parameters of rectifier systems forming the basic equipment of the substations in question *with this sentence structure – it is unclear exactly what this is an example of – this needs rephrasing*. Further studies and analyses of traction load details should aid the development of load description tools to better perform engineering calculations. The development of engineering tools to better *'better' is very vague and subjective – for the sake of clarity, consider choosing something more specific and objective* describe possible traction loads of improved power supply units is a comprehensive task. One of the aspects of key importance in this regard is presented below

2. Particulars of loads occurring in the traction sub-station concerned

The registered loads taken to analysis and described to some extent below occurred to the tramway traction substation located almost in the middle of a large city with a rail and road traffic hub of high traffic density [5, 9–11]

2.1. Examples of momentary traction load values

Figure 1 shows some graphs of momentary traction current values which occurred in the rectifier units of the abovementioned tramway traction substation. One normal working

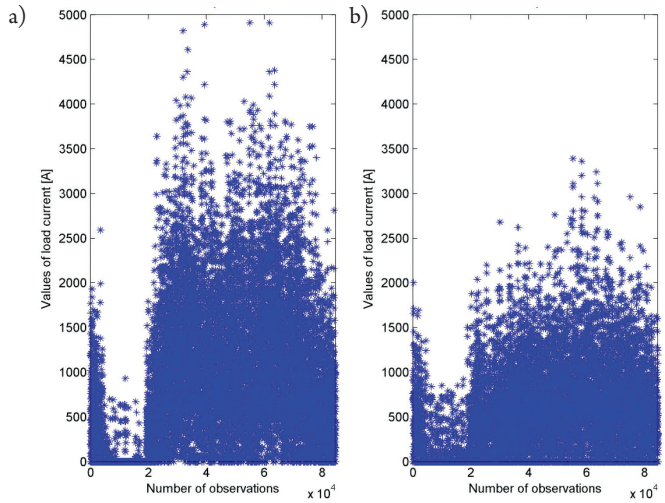

Fig. 1. Registered momentary values of load current in the 'Czyżyny' traction substation on: a) 23rd Oct 2013 (Wed), b) 27th Oct 2013 (Sun) [5, 11, 22]

day (23rd Oct 2013 – Wednesday) and one public holiday (27th Oct 2013 – Sunday) were considered for the presentation. The provided results refer to two days which cover approx. 0.55% of the calendar year, and currently used engineering tools are based on the assessment of annual power consumption. Much longer periods of time are considered later in this paper.

These results show that the 'Czyżyny' traction substation was not fully loaded within the considered days [5, 11]. For example, the load applied to the substation was equal to the continuous power of the four rectifier units the substation is equipped with for a total of only six minutes and the substation (rectifier units) remained load free for a total duration of almost five hours within the working day. All four transformers of the rectifier units consumed power from the grid within this time only to cover idle running losses.

2.2. Examples of momentary traction load values

The measurement results provided in this section of the paper and selected aspects of their analysis refer to the period of time [9, 22] covering sixteen consecutive calendar weeks within an autumn and winter season (from 1st Sept 2014 to 21st Dec 2014). Some parts of the submitted results were subsequently subject to analysis performed using artificial neural networks (Chapter 3). Figure 2 shows the average values of traction load currents occurring in the individual weeks of the test period.

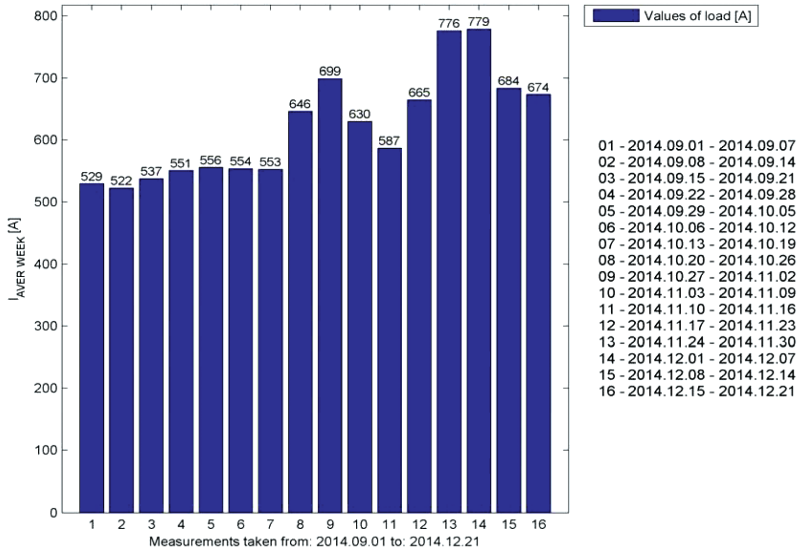

Fig. 2. Average values of traction load currents occurring in the individual weeks [9]

The above figure shows that the substation was subject to a varying load during the individual weeks of the test period. The highest average current value (i.e. the largest power consumption) occurred during the 14th week and amounted to 778.74 A, which is 1.25 times more than the average current value for this period (621.61 A).

Figure 3a shows the average values of traction load current occurring on the individual days (with a 24-hour period); Figure 3b shows a graph of these loads in a descending order, from the highest value (965.38 A) to the lowest value (304.11 A).

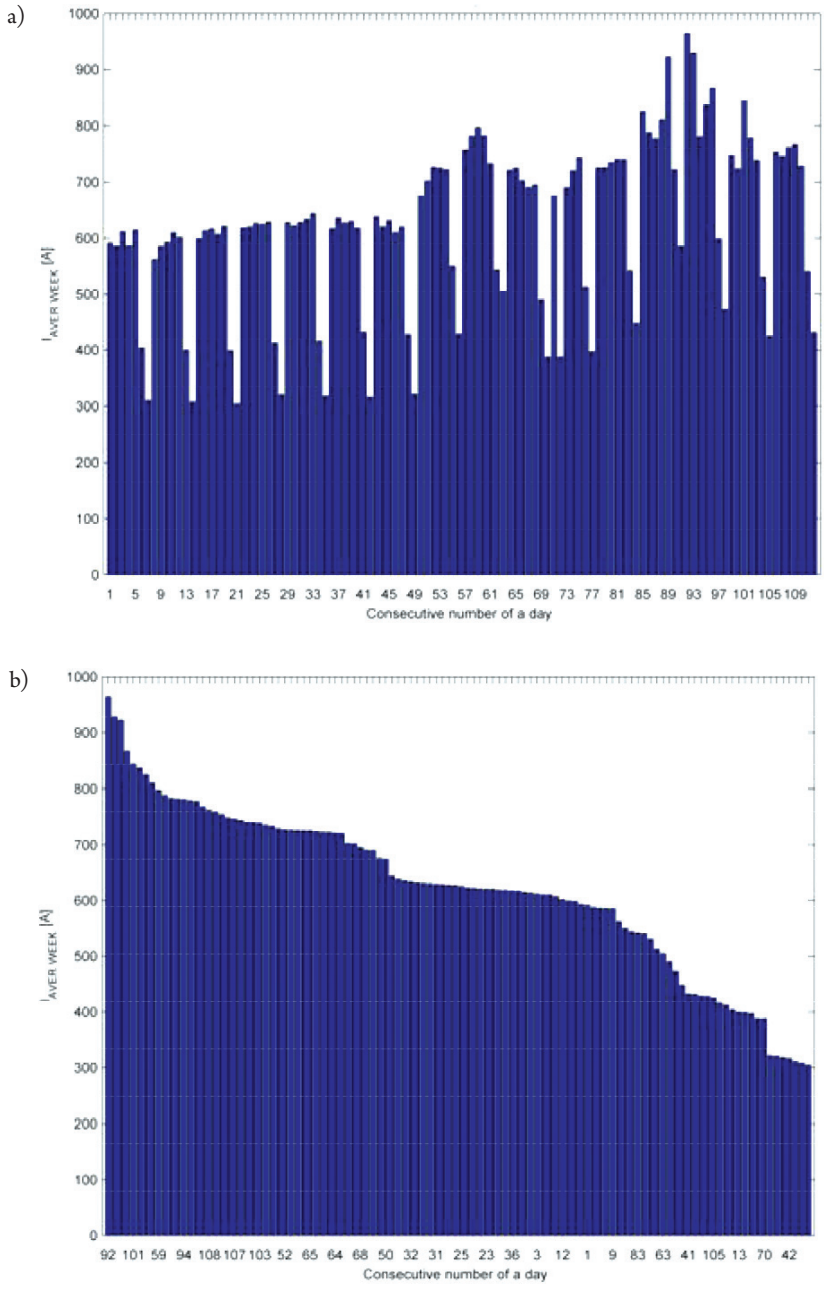

Fig. 3. Average values of traction load currents occurring on individual days:a) in the order in which they occurred, b) in descending order [9]

Additional figures show the graphs of momentary values of load currents occurring in the traction units selected by the following criteria:

- Figure 4 shows the graph of maximum average current value occurring within a five-minute timespan of all five-minute timespans within the 112 analysed days,
- Figure 5 shows the graph of current occurring within a five-minute timespan among all five-minute timespans in the 24-hour period in which the five-minute overload factor was the highest,
- Figure 6 shows the graph of maximum average current values occurring within a sixty-minute timespan of all sixty-minute timespans within the 112 analysed days,
- Figure 7 shows the graph of current occurring within a sixty-minute timespan among all sixty-minute timespans in the 24-hour period in which the sixty-minute overload factor was the highest.

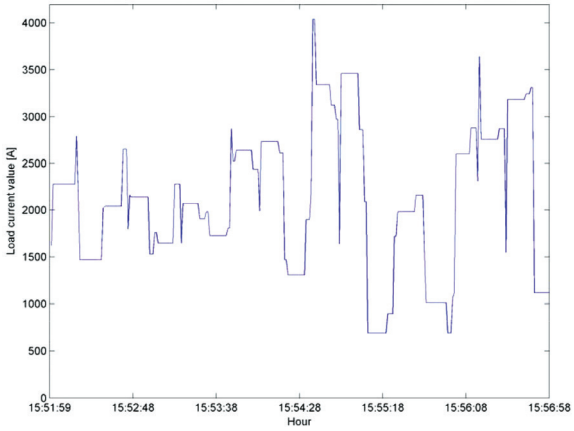

Fig. 4. The graph of load current for a 5-min. timespan in the day (24 hr) within which the maximum 5-min. overload falls (the authors' own elaboration)

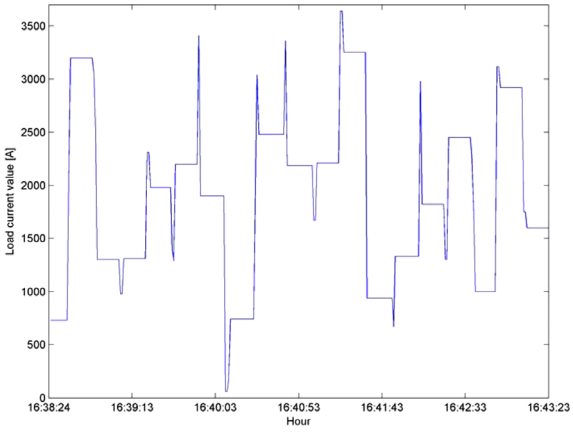

Fig. 5. The graph of load current for a 5-min. timespan in the day (24 hr) within which the maximum 5-min. overload falls (the authors' own elaboration)

For the purposes of this section, the overload is the ratio of the maximum average current value in the given timespan (either 5 or 60 mins) and the average current value in the given day (24-hour period). This factor is designated by the authors as 'α'.

Quantitative comments to the graphs plotted in the above figures are provided in Table 1.

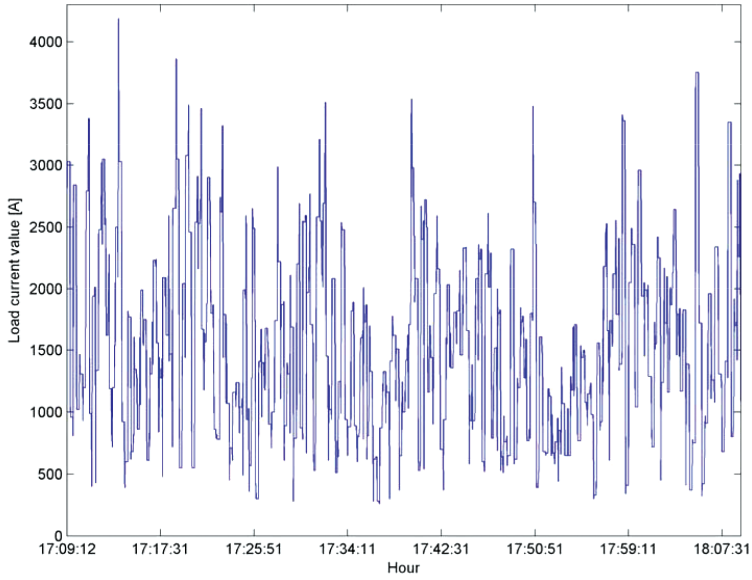

Fig. 6. The graph of load current for a 60-min. timespan in the day (24 hr) within which the maximum 60-min. overload falls (the authors' own elaboration)

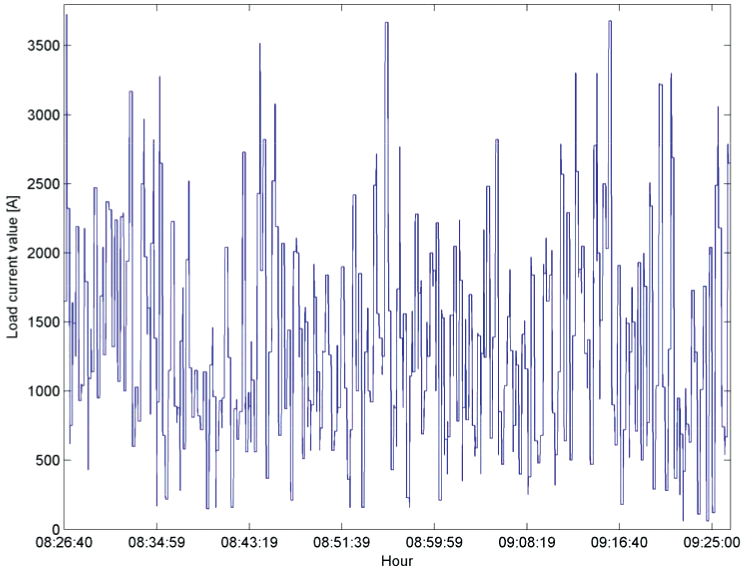

Fig. 7. The graph of load current for a 60-min. timespan in the day (24 hr) within which the maximum 60-min. overload falls (the authors' own elaboration)

Table 1. Parameters for graphs of loads for the 5- and 60-min. timespans within the days (24 hr) of highest and maximum loads within the selected span (the authors' own elaboration)

Item	Timespan	Determinant	Consecutive day number	Date	Time of occurrence	Max. value [A]	Average value [A]	Effective value [A]	Form coefficient [-]	Peak coefficient [-]
1.	5 min	Maximum load	89	28/11/2014	15:51:59 15:56:58	4,040	2,126	2,260	1.0630	1.7873
2.	5 min	Maximum overload factor	18	18/09/2014	16:38:24 16:43:23	3,640	1,890	2,048	1.0835	1.7767
3.	60 min	Maximum load	92	01/12/2014	17:09:12 18:09:11	4,190	1,518	1,686	1.1100	2.4851
4.	60 min	Maximum overload factor	43	13/10/2014	08:26:40 09:26:40	3,730	1,327	1,518	1.1436	2.4566

The above figures show that in-spite of noticeable fluctuations, the traction load currents did not fall to zero. Figure 3 demonstrates the highest average value of traction load occurring within day 92 (1st Dec 2014). Table 1 also shows that, for example, the 60-min. timespan with the highest average load value of all 112 analysed days (Fig. 6) also falls on day 92; this occurred in the late afternoon (17:09:12 – 18:09:11).

The other three cases indicated in Table 1 fell on the other days in which the load was lower than the load which occurred on day 92. This observation as well as the other results provided in the table additionally confirm that the traction load fluctuates and is of a complex nature.

Further studies on this matter should enable better investigation of the properties and nature of traction loads. The results obtained should facilitate the development of better engineering tools and/or new solutions for DC traction power supply units [14].

3. Introductory information and input data

The calculations were performed using Matlab version R2011B. The input data for the ANN analysis was 112 pairs of numbers. In each pair, one of the numbers (input) was the temperature value and the other number (output) was the substitute thermal factor corresponding to the temperature.

Measurement data processing was performed using a two-layer feedforward neural network implemented in Matlab. Figure 8 shows the neural network block created in the Simulink environment.

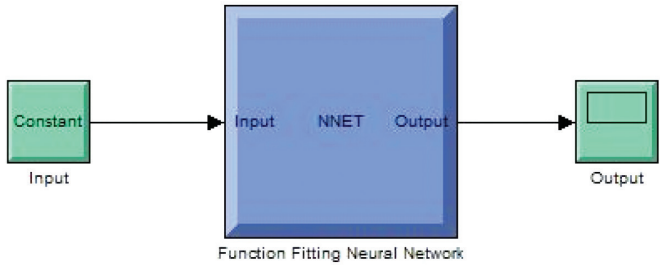

Fig. 8. The neural network block created in the Simulink environment; own work

Figure 9 depicts the created neural network structure. This structure had one hidden layer consisting of four neurons. There were no delays implemented on the input for this layer. The activation function for the hidden layer was tangensoidal (tansig). The output layer had a linear activation function.

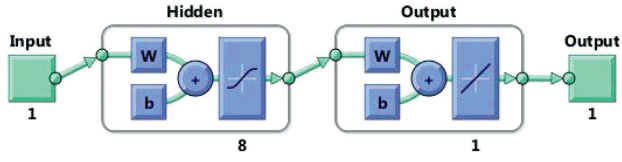

Fig. 9. The created neural network structure; own work

The aim of the study was to approximate the function that would relate the temperature factor value for each thermal coefficient corresponding to the temperature.

The results shown below in Section 4 were obtained for the following ANN training settings:

- maximum number of epochs to train: 1000
- performance goal: 0
- learning rate: 0.01
- maximum validation failures: 12
- momentum: 0.9
- minimum performance gradient: 10^{-10}
- epochs between displays: 25
- maximum time to train in seconds: infinite

In order to teach the designed artificial neural network, one-way network (up to three layers) training was used according to the Leveneberg-Marquardt algorithm.

4. Computation

Figure 10 depicts results obtained from the training, validation and test of the ANN in the form of an error histogram.

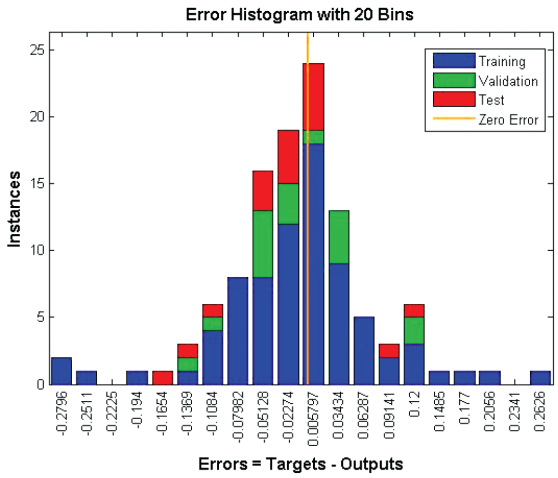

Fig. 10. Error histogram (own work)

Figure 11 presents an illustration of the performance of the ANN for successive learning epochs.

Figure 11 presents the artificial neural network performance graph during learning. The ordinate axis refers to the ANN performance function values. The mean square error ('MSE') was chosen as the performance function. The horizontal axis corresponds to learning epochs. The system reached the best neural network validation of the ANN performance for the fifth epoch and it was *'4.5551'*·10^{-3}. One can observe that the neural network system continued the

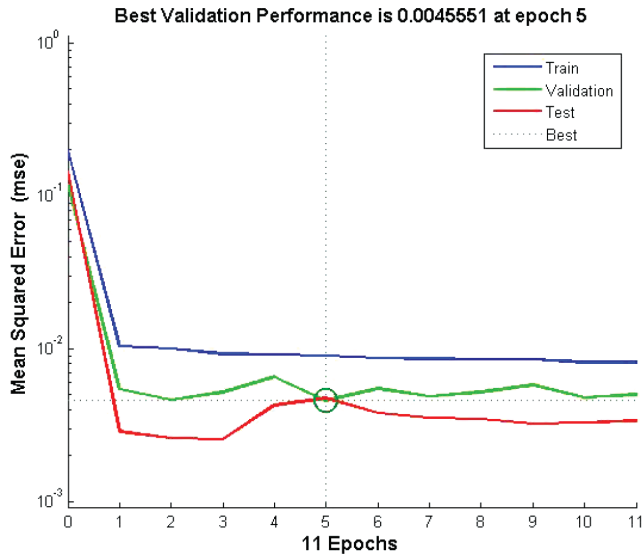

Fig. 11. Performance of the ANN (own work)

learning algorithm for another twelve epochs in order to confirm the alleged local minimum for the goal set for the created network structure (Fig. 9). From epoch 1 to 5, a downward trend in validation tests of the ANN learning can be seen.

Figure 12 depicts the regression results for the training, validation and test, and the regression for all data assigned to the ANN learning with a supervisor. Here, the ordinate axis represents the neural network output for the given input data. The abscissa axis shows values from the actual measurements (targets), to which the values returned by the ANN should be convergent.

The R = 1 regression result means that there is an unequivocal relationship between the actual value (target – from measurement or simulation) and the neural network output value.

The regression results for the discussed case are as follows. The regression for the data assigned to the training reached R = 0.69866. The data constituted about 70% of all data assigned to the ANN learning with a supervisor. The regression for the validation was R = 0.80432. The data used for this step were about 15% of all data. Lastly, the regression for the test was R = 0,74238. Consequently, the data used in this stage was about 15% of all data. One more regression value was calculated; this represents all data and was R = 0.7109.

The training, validation and test are performed during the procedure of neural network learning.

Figure 13 presents the results obtained from the approximation process (function fitting process) performed by artificial neural network learning. In this figure, dots represent the actual values of the substitute thermal factor obtained from measurements (targets), while cross marks represent the results of the approximation. Vertical lines indicate absolute errors between actual values and the corresponding results obtained by the function fitting process. The solid line is the plot of the resulting approximating function.

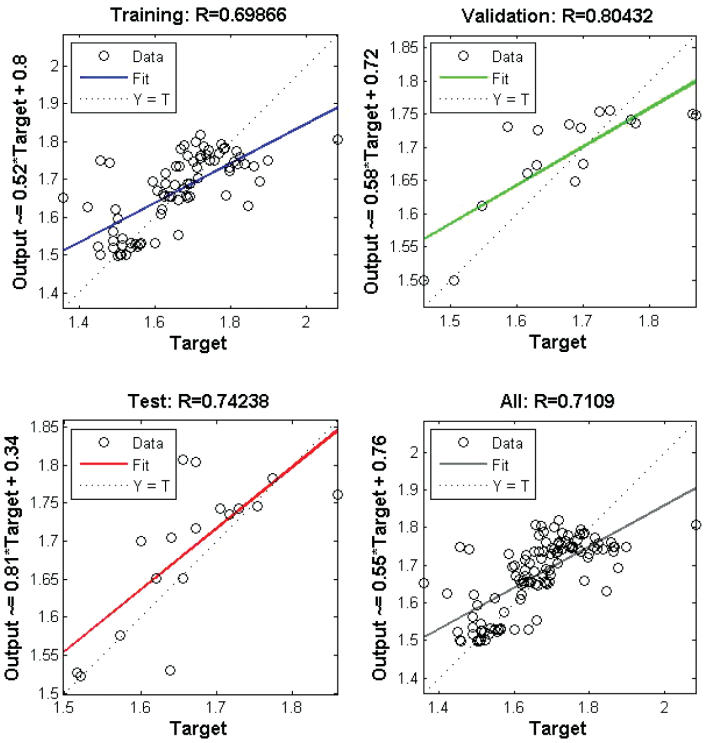

Fig. 12. Regression results for the training, validation and test and the regression for all data assigned to the ANN learning with a teacher (own work)

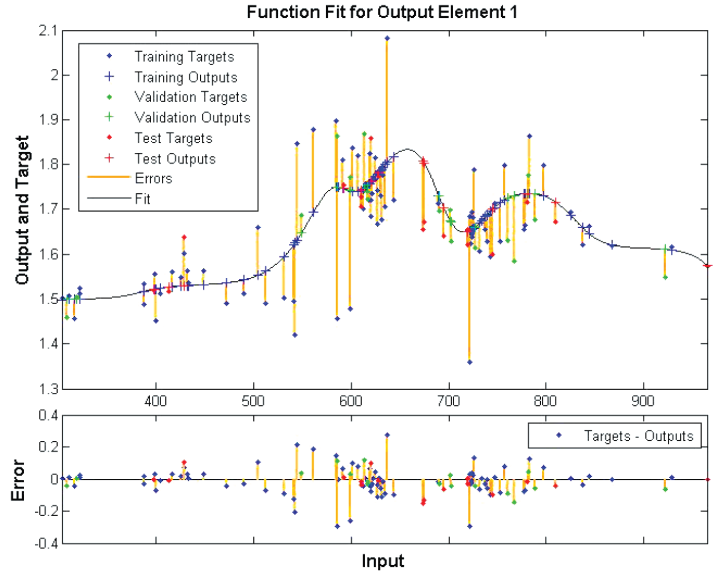

Fig. 13. Results of function fitting with the use of the ANN; output – substitute thermal factor; input – the temperature (Own work)

5. Summary

The results of the analysis relating to the character of the overload conditions of the traction substation using neural networks allow continuous development itself. Compared to previous articles [12], the data presented in this paper has improved consider stating how it has improved; this is because it is based on a new model of SSN. This is an example of regression calculated for all of the measurement data. In the article [12], the value of that regression was R = 0.68304, now it is R= 0.72248. The improvement was achieved by extension (more neurons) of the hidden layer.

The presented studies imply the necessity to conduct further research across a wider range. Authors in subsequent articles will undertake analyses of the influence of the structure on the results achieved through modelling the phenomenon.

References

[1] Białoń A., Chrabąszcz I., Hudym W., Kaczmarczyk A., Prusak J., Wpływ odległości kolejowych podstacji trakcyjnych na rozkład obciążeń między nimi – symulacyjna ocena wybranych przypadków, TTS Technika Transportu Szynowego, 7-8/2015, 80–82.

[2] Chrabąszcz I., Drapik S., Dudzik M., Kaczmarczyk A., Prusak J., *Analiza obciążeń zespołów prostownikowych, dla „inteligentnych" kolejowych podstacji trakcyjnych DC – wstępne badania symulacyjne wybranych przypadków*, Logistyka 6/2015, 990–999.

[3] Chrabąszcz I., Prusak J., Drapik S., *Trakcja elektryczna prądu stałego. Układy zasilania.* Podręcznik INPE dla elektryków, Zeszyt nr 27, Kraków – Bełchatów, 2009.

[4] Drapik S., Dudzik M., Kobielski A., Prusak J., *Komparatywna ocena zmienności obciążeń kolejowych podstacji trakcyjnych.* 11th International Conference „Modern Electric Traction" MET'2013, Poland Warsaw, October 10 – 12. 2013; materiały konferencyjne, 62–67.

[5] Drapik S., Kaczmarczyk A., Kobielski A., Prusak J., *Charakter zmienności obciążeń tramwajowych podstacji trakcyjnych zasilających linie o różnej specyfice ruchu pojazdów*, TTS Technika Transportu Szynowego, 6/2015, 43–48.

[6] Drapik S., Kobielski A., Prusak J., *Fluktuacja obciążeń podstacji trakcyjnych w ujęciu teorii szeregów czasowych.* TTS Technika Transportu Szynowego, 7–8/2010, 59–64.

[7] Drapik S., Kobielski A., Prusak J., *Selected issues of traction substation load* variability, Chapter 5, 47–58, Monografia Politechniki Gdańskiej Modern Electric Traction, Power Supply, Edited by Krzysztof Karwowski, Adam Szeląg, Gdańsk University of Technology, Faculty of Electrical and Control Engineering, Gdańsk 2009.

[8] Drapik S., Kobielski A., Prusak J., *Wybrane aspekty zmienności obciążeń kolejowych podstacji trakcyjnych.* TTS Technika Transportu Szynowego 4/2010, 27–31.

[9] Drapik S., Kuzniecow W., Markowski P., Prusak J., Woszczyna B., *Badanie skali zmienności obciążeń wybranej tramwajowej podstacji trakcyjnej na podstawie rzeczywistych wyników pomiarowych dla spójnego okresu czasowego obejmującego szesnaście tygodni*, Logistyka 6/2015, 1026–1035.

[10] Drapik S., Markowski P., Prusak J., Woszczyna B., *Analiza obciążeń zespołów prostownikowych przed i po wystąpieniu przeciążenia na przykładzie wybranej tramwajowej podstacji trakcyjnej*, TTS Technika Transportu Szynowego, 12/2015, 427–434.
[11] Drapik S., Markowski P., Prusak J., Woszczyna B., *Tramwajowe podstacje trakcyjne – wybrane problemy bezpieczeństwa ekologicznego w świetle oceny ich obciążeń*, Logistyka 4/2015, 3017–3027.
[12] Dudzik M., Drapik S., Prusak J., *Approximation of overloads for a selected tram traction substation using artificial neural network algorithms*, not published.
[13] Hilgard E.R., *Wprowadzenie do psychologii*, Państwowe Wydawnictwo Naukowe, Warszawa 1973.
[14] Jagiełło A.S., Chrabąszcz I., Drapik S., Dudzik M., Kobielski A., Prusak J., *System do aktywnej regulacji obciążenia zespołów prostownikowych kolejowej podstacji trakcyjnej. Sposób aktywnej regulacji obciążenia zespołów prostownikowych kolejowej podstacji trakcyjnej*, Rozwiązanie zarejestrowane w Urzędzie Patentowym RP na rzecz Politechniki Krakowskiej pod numerem P.511511,objęte ochroną prawną od dnia 10.03.2015.
[15] Kałuża E., Bartodziej G., Ginalski Z., *Układy zasilania i podstacje trakcyjne*, Skrypty uczelniane Politechniki Śląskiej nr 1220, Gliwice, 1985
[16] Kobielski A., Drapik S., Dudzik M. Prusak J., *Time Series as an Aid to Research of traction Substation Load*, JEPE Journal of Energy and Power Engineering, Volume 7, Number 5, May 2013 (Serial Number 66), David Publishing Company, El Monte, USA, 979–986.
[17] Kobielski A., Drapik S., Dudzik M., Prusak J., *Niektóre problemy analizy i modelowania zmienności obciążeń kolejowych podstacji trakcyjnych*, Monografia 450: Elektrotechnika w Zastosowaniach Trakcyjnych; seria: Inżynieria Elektryczna i Komputerowa, edited by A.S. Jagiełło, Politechnika Krakowska, Kraków 2014, 237–249.
[18] Kobielski A., Drapik S., Dudzik M., Prusak J., *Wstępne studium efektywności zastosowania sieci neuronowych w badaniach obciążeń kolejowych podstacji trakcyjnych*, TTS Technika Transportu Szynowego, 10/2014, 40–43.
[19] Korbicz J., Obuchowicz A., Uciński D., *Sztuczne sieci neuronowe. Podstawy i zastosowania*, Akademicka Oficyna Wydawnicza PLJ, Warszawa 1994.
[20] Mierzejewski L., Szeląg A., Gałuszewski M., *System zasilania trakcji elektrycznej prądu stałego*, Wydawnictwo Politechniki Warszawskiej, Warszawa 1989.
[21] Tadeusiewicz R., *Sieci neuronowe*, Akademicka Oficyna Wydaw. RM, Kraków 1992.
[22] Wyniki pomiarów prądów obciążeń trakcyjnych kabli zasilających podstacji tramwajowej nr „01" („Czyżyny"), materiały udostępnione przez ZIKiT w Krakowie, 2015.